

## ABSTRACT

### Using Sycamore Leaves to Reconstruct Ancient Light Environments

Desirae E. Thorne, M.S.

Mentor: Daniel J. Peppe, Ph.D.

Light environments strongly influence the composition and structure of terrestrial ecosystems and climates. Further, light intensity impacts both a plant's leaf morphologic traits and its chemical composition, making it possible to quantify how these variables change in response to light intensity. Thus, it is possible to use leaf morphology and chemical composition to reconstruct ancient light environments, which can provide critical insights into past environments. Here, we present results focused on the development of a proxy for light availability using leaf size and shape (physiognomy) and chemical composition from modern Sycamore leaves that were grown under varying degrees of light availability in an outdoor light experiment. We found notable differences in leaf physiognomic variables, such as leaf area and perimeter, across light environments; and results from  $^{13}\text{C}$  NMR spectroscopy also indicate differences between light environments, with more abundant in lipids and less abundant in lignin found in low light conditions. Physiognomic and geochemical data were used to develop three different multivariate models for predicting daily light integral (DLI) that can applied to the fossil record. Using these models, we analyzed early Paleocene *Platanites* fossil leaves from the San Juan

Basin, New Mexico to reconstructed ancient light conditions to help understand light availability and its impacts on the ecosystem and plant communities of early Paleocene.

Using Sycamore Leaves to Reconstruct Ancient Light Environments

by

Desirae E. Thorne, B.S.

A Thesis

Approved by the Department of Geosciences

---

Joe Yelderman, Ph.D., Chairperson

Submitted to the Graduate Faculty of  
Baylor University in Partial Fulfillment of the  
Requirements for the Degree  
of  
Master of Science

Approved by the Thesis Committee

---

Daniel J. Peppe, Ph.D., Chairperson

---

William C. Hockaday, Ph.D.

---

Joseph D. White, Ph.D.

Accepted by the Graduate School

May 2023

---

J. Larry Lyon, Ph.D., Dean

Copyright © 2023 by Desirae E. Thorne

All rights reserved

## TABLE OF CONTENTS

|   |      |
|---|------|
| LIST OF FIGURES .....   | vii  |
| LIST OF TABLES .....  | viii |
| ACKNOWLEDGMENTS .....   | ix   |
| CHAPTER ONE .....   | 1    |
| Introduction.....   | 1    |
| CHAPTER TWO .....   | 5    |
| Methods .....   | 5    |
| Modern Sycamore Leaves.....   | 5    |
| Fossil Leaf Collection .....  | 5    |
| Leaf Physiognomic Measurements .....  | 6    |
| Solid-State <sup>13</sup> C Nuclear Magnetic Resonance .....                                | 7    |
| δ <sup>13</sup> C Stable Isotopic Analysis .....  | 8    |
| Statistical Analysis.....   | 9    |
| CHAPTER THREE .....   | 10   |
| Results.....  | 10   |
| Leaf Physiognomic Response to Light Environment .....                                       | 10   |
| Leaf Molecular Structure Response to Light Environment .....                                | 14   |
| Leaf δ <sup>13</sup> C Response to Light Environment .....                                  | 17   |
| Predictive DLI Linear Regression .....  | 17   |
| Reconstructed DLI from Fossil Platanites .....  | 18   |
| CHAPTER FOUR.....   | 20   |
| Discussion.....   | 20   |
| Influences on Leaf Traits: Climate, Light Quantity, Light Quality .....                     | 20   |
| Developing Multivariate Models for Predicting Light Intensity using Modern<br>Platanus..... | 23   |
| Predicted DLI at Fossil Sites and Interpretation of Light Environment .....                 | 24   |
| CHAPTER FIVE .....  | 27   |
| Conclusions.....  | 27   |

|                   |    |
|-------------------|----|
| APPENDIX.....     | 29 |
| BIBLIOGRAPHY..... | 35 |

## LIST OF FIGURES

|  |    |
|--|----|
| Figure 3.1. Relationship between light treatment and leaf physiognomic traits.....     | 20 |
| Figure 3.2. Relationship between light treatment and leaf physiognomic traits.....     | 21 |
| Figure 3.3. Relationship between light treatment and leaf molecular components. ....   | 24 |
| Figure 3.4. Relationship between light treatment and leaf $\delta^{13}\text{C}$ . .... | 25 |

## LIST OF TABLES

|   |    |
|---|----|
| Table 3.1. Regression models for predicting daily light integral (DLI). ..... | 28 |
|---|----|

## ACKNOWLEDGMENTS

I would like to thank Baylor's University Research Committee, the National Science Foundation, the Dallas Paleontological Society and the Department of Geosciences at Baylor University for providing financial support to conduct this project. To my advisor Dr. Daniel Peppe, thank you for your continuous support and encouragement throughout the duration of this project. To Danielle Gygi, my dear friend, thank you for being my mentor and big sister. A special thanks to Vinothan Sivapalan and Ashleigh Browne for their assistance with NMR analyses. To Dr. Ren Zhang, thank you for running the IRMS for our isotopic analyses. Additional thanks to Dr. Andrew Flynn, Dr. Emily Beverly, and Dr. Joseph Milligan for your guidance while in the field. Thank you to Jie Geng for being a great partner and leader in the field and to Jiaxun Liu, who served as our undergraduate field assistant. To my committee members, Dr. William Hockaday and Dr. Joseph White, thank you for all of your support and feedback on this project.

## CHAPTER ONE

### Introduction

Light is a critical component to plant life, and different light characters, such as wavelength, intensity, direction, and duration, vary and impact plant development in numerous ways. In particular, plant morphology and chemical composition are affected by light intensity (e.g., Poorter et al., 2019). An important species-specific characteristic of juvenile trees is their ability to adapt their morphological and architectural traits based on light availability (Messier et al., 1999). Additionally, differences in isotopic composition and abundances of specific molecular components with light availability have been observed in plants (e.g., Poorter et al., 2006; Milligan et al., 2021; Wang et al., in progress). Furthermore, at the ecosystem level in terrestrial environments, light also influences structure, composition, and climate (e.g., Betts et al., 1997; Asner et al., 2003). The light-dependency of certain plant traits has allowed paleobotanists to categorize leaves in the fossil record based on their light environment (e.g., Kürschner, 1997; Xiao et al., 2011, Milligan et al., 2021) and to reconstruct canopy structure of ancient ecosystems (Dunn et al., 2015; Graham et al., 2019). If we can measure and quantify the aforementioned developmental changes with varying light intensity in modern plants, we have the potential to learn about light regimes in ancient ecosystems, which has important implications for understanding ancient plant communities.

In modern closed-canopy forests, a pattern in the carbon isotopic composition ( $\delta^{13}\text{C}$ ) of leaves has been observed, in which these values decline downward from the top

of the canopy to the forest floor (e.g., Vogel, 1978; Graham et al., 2014; Graham et al., 2019). For this reason, the carbon isotopic composition of leaves has been used to distinguish environmental conditions (i.e., light conditions and canopy structure) from which those leaves are sourced (Farquhar et al., 1989; Graham et al., 2019; Cheesman et al., 2020). Generally speaking, leaves that are exposed to less sunlight are depleted in  $\delta^{13}\text{C}$  compared to leaves that are exposed to more sunlight. Not only has this phenomenon been observed in closed-canopy forest ecosystems, but it has also been observed in light experiments (Lynch et al., 2012) and within the crown of a single tree (Le Roux et al., 2012; Xiao et al., 2013). Leaf  $\delta^{13}\text{C}$  differs because of increased isotopic discrimination at low light caused by a reduction in the rate of photosynthesis and an elevated ratio of internal to external  $\text{CO}_2$  concentration (Farquhar et al., 1989). Within a closed-canopy system, other factors leading to these isotopic differences include vertical gradients in light, humidity, atmospheric  $\text{CO}_2$  concentration, and  $\delta^{13}\text{C}$  of the atmosphere, which lead to the “canopy effect” (e.g., Graham et al., 2014). Graham et al. (2019) used this information to distinguish between open and closed canopies in the fossil record. Additionally for fossil leaves, some studies have observed differences in  $\delta^{13}\text{C}$  between sun and shade morphotypes (Turney et al., 2002; Nguyen Tu et al., 2004; Xiao et al., 2013; Milligan et al., 2021). However, these differences are not always statistically significant (e.g., Xiao et al., 2013).

Following the classes of molecular components described by Baldock et al. (2004), some studies have also found differences in the abundance of different components (protein, carbohydrates, lignin, lipids) with changes in the levels of irradiance to which leaves are exposed (Waring et al., 1985; Mooney et al., 1995; Niinemets et al., 1999; Evans and Poorter, 2001). For example, leaves of plants grown in low light conditions have been

found to have lower concentrations of carbohydrates and lignin (Waring et al., 1985; Mooney et al., 1995, Niinemets et al., 1999). On the other hand, protein abundances have been found to be higher with lower light conditions (Evans and Poorter, 2001). These different molecular components within plants are associated with unique biosynthetic pathways and construction costs, and there is an observed difference in the biologic costs associated with levels of irradiance experienced by the plants (Poorter et al., 2006). Additionally, Wang et al. (in progress) found that the average chain length (ACL) of leaf wax n-alkanols in *Quercus buckleyi* were strongly correlated with absorbed photosynthetically active radiation (APAR), which is possibly related to genetic regulation of biosynthetic responses to seasonal variations in temperature and light stresses.

At the leaf cell level, differences in cellular morphology have been observed with changes in light level (Watson, 1942; Hectors et al., 2010; Wagner-Cremer et al., 2010; Dunn et al., 2015; Carins Murphy et al., 2016; Wang et al., 2018; Cheesman et al., 2020; Milligan et al., 2021). Leaves from plants grown in low-light environments, for example, have larger epidermal cells (Watson, 1942) and their anticlinal cell walls are more undulated compared to leaves from plants grown in higher light environments (Watson, 1942; Carins Murphy et al., 2016). In general, sun leaves are typically found to have smaller cells with less cell wall undulation, and this relationship between cell wall undulation and light has been called the undulation index (UI, Kürschner, 1997). Several studies have since found utility in using UI to differentiate between sun and shade morphotypes for a variety of plant taxa from the fossil record (Kürschner, 1997; Wu et al., 2009; Xiao et al., 2011; Bush et al., 2017; Wang et al., 2018; Milligan et al., 2021).

However, species-specific responses in UI exist, which may lead to discrepancies in the inferred degree of canopy closure, and in turn, light environments (Bush et al., 2017).

At the leaf level, physiognomy (i.e., size and shape) has been a useful metric in developing several different paleoenvironmental and paleoecological proxies (see review in Peppe et al., 2018). However, despite there being clear qualitative differences in the physiognomy of modern leaves based on the light environment they experienced during growth (e.g., Milligan et al., 2021), there have not been many attempts to quantify and use these differences in leaf physiognomy to assess light environments in ancient forests.

Here we assess the response of leaf physiognomy, stable isotopic composition, and molecular component abundances to different light regimes in the modern sycamore species *Platanus occidentalis*. Our study uses modern sycamore leaves grown under different light regimes and builds on the work of Milligan et al. (2021), who quantified the responses of cuticle morphology (cell wall undulation, cell size) and carbon isotopes in *P. occidentalis* to changes in light conditions. We then used the relationships between physiognomic, isotopic, and molecular variables and daily light integral (DLI) to develop multivariate models for estimating DLI in the fossil record and apply it to an early Paleocene fossil leaf site from the San Juan Basin, New Mexico.

## CHAPTER TWO

### Methods

#### *Modern Sycamore Leaves*

Physiognomic and geochemical data were collected from *Platanus occidentalis* leaves that were grown in a field shade cloth experiment carried out in 2018 at the Lake Waco Wetlands in Waco, Texas (Milligan et al., 2021). The field shade cloth experiment consisted of six, 3.0 x 3.0 m plots, with five saplings of *P. occidentalis* planted within each plot. Five of the plots were surrounded by a PVC structure covered by different types of shade cloth: 30%, 60%, 90% black neutral-density cloth and 60% and 87% green cloth. The final plot remained uncovered, serving as the control for the experiment. One to two leaves were collected from each sapling per light treatment at the end of the experiment ( $N = 9-10$  per light treatment), making a total of 59 leaves analyzed in this study.

#### *Fossil Leaf Collection*

Fossil *Platanites* leaves were collected from fossil localities within the early Paleocene Nacimiento Formation in the San Juan Basin, New Mexico. We specifically targeted previously discovered sites that contained *Platanites* fossil leaves abundant in cuticles (e.g., Flynn, 2020; Milligan, 2022). During our collection we focused on collecting mostly complete leaves and leaves with preservation of cuticle allowing us to make both physiognomic and geochemical measurements on multiple leaves from the same site. The site we focus on here is in the De-Na-Zin Wilderness Area (DP-1304). This sites age was

calculated to be  $65.33 \pm 0.05$  Ma using sediment accumulation rates based on the local stratigraphic position of magnetostratigraphic boundaries (Flynn, 2020; Flynn et al., 2020).

### *Leaf Physiognomic Measurements*

We measured different foliar characteristics using the digital leaf physiognomy (DiLP) outlined by Royer et al. (2005) and Peppe et al. (2011). Briefly, we utilized the following protocol. We photographed each leaf, along with a cm scale bar, against a black background for maximum contrast and conducted image preparation using Adobe Photoshop (Adobe Systems, San Jose, California, USA). First, the leaf was copied as a new layer. The petiole was removed from the leaf in this new layer. We then repaired any minor portion of the leaf margin that was damaged by reconstructing those segments using straight lines. The leaf was then copied again as a third layer, where the teeth were removed from sinus to sinus. In some cases where the leaf was fragmentary or the margin was damaged, additional steps were necessary, and in those cases, we followed the methods of Peppe et al. (2011) for processing and measuring incomplete leaves. For example, if only half of a leaf could be reliably reconstructed, and the leaf was symmetrical, measurements were doubled based on measurements for one half of the leaf. Additionally, many of the leaves had folds in them which could not be unfolded without breakage occurring since they had been pressed and dried. In those cases, the folds were repaired digitally allowing us to measure the complete leaf. Following image preparation, measurements were made using ImageJ (<http://rsbweb.nih.gov/ij/>).

### *Solid-State <sup>13</sup>C Nuclear Magnetic Resonance*

A total of 30 samples were analyzed using <sup>13</sup>C NMR. We combined leaves from each tree sampled from the Milligan et al. (2021) field shade cloth experiment. *P. occidentalis* leaves were sub-sampled by cutting out three ~1 in<sup>2</sup> pieces from each leaf, taking care to cover three distinct areas from the midvein to the margin of the leaf. To prevent contamination, samples were collected wearing vinyl gloves and the cutting blade was cleaned with alcohol prior to cutting each leaf. Each NMR sample consisted of 6 subsamples from 1-2 different leaves per tree, which were placed in labeled aluminum weighing boats. A small amount of liquid nitrogen was poured into a clean aluminum mortar and allowed to dissipate, then a sample was added and crushed using an aluminum pestle. Samples were then transferred back into their respective aluminum weighing boats and placed in an oven to dry overnight at ~40°C. Once samples were dry, they were packed into rotors for analysis. Fossil leaves were sampled by scraping the surface gently with dental tools, avoiding the inclusion of matrix material. The organic material scraped off was then collected in a labelled glass vial.

<sup>13</sup>C NMR analysis was conducted using a standard bore 300 MHz Bruker Avance III spectrometer (4 mm magic angle spinning (MAS) and frequency of 12 kHz). Spectra were acquired with a variable amplitude cross-polarization (CP) sequence with composite pulse decoupling (TPPM15) during signal acquisition. An additional dipolar dephasing experiment was conducted for fossil leaves. The functional groups present in the samples and their abundances were found by calculating the peak areas. The chemical shift regions used were as follows: Alkyl, 0–45 ppm; N-Alkyl + Methoxyl, 45–60 ppm; O-Alkyl, 60–95 ppm; Di-O-Alkyl or Alkene, 95–110 ppm; Aryl (aromatic), 110–145 ppm; O-Aryl

(phenolic), 145–165 ppm; Amide + Carboxyl, 165–190 ppm; and Ketone, 190–215 ppm. The specific molecular components and their abundances were found by integrating the peak areas into the terrestrial molecular mixing model of Baldock et al. (2004). This model uses the integrated peak data acquired via  $^{13}\text{C}$  NMR to predict the molecular composition of the sample. The molecular components include carbohydrate, protein, lignin, lipid, carbonyl, and char (Baldock et al., 2004). For the modern leaves, we assumed there was no char component and applied the 5-member model which excludes char. For fossil leaves, we applied the 6-member mixing model, which includes char (Baldock et al., 2004).

### *$\delta^{13}\text{C}$ Stable Isotopic Analysis*

Prepped samples used for NMR were also used to conduct  $\delta^{13}\text{C}$  stable isotopic analysis on modern leaves. 2 mg of each sample was weighed out and placed into tin capsules. Capsules were tightly sealed and placed into a holder where their name, mass, and slot number were noted. Isotope ratio mass spectrometry (IRMS) was conducted using the Delta-V Advantage mass spectrometer (Thermo Fisher Scientific, Waltham, MA, USA) in the Stable Isotope Laboratory at Baylor University. A total of 30 modern samples were analyzed for their  $\delta^{13}\text{C}$  values. Fossil leaves were sampled by scraping the surface gently to collect cuticle material without the inclusion of matrix material. This material underwent a sequential HCl/HF treatment, adopted from Gelinas et al. (2001). The cuticle was submerged in HCl (36.5-38%) to remove carbonate and rinsed in distilled water, it was then treated with HF (48%) to dissolve silicates and rinsed in distilled water again. Finally, it was oven dried at 60°C prior to being placed in capsules for analyses.

### *Statistical Analysis*

Statistical analysis on all physiognomic and geochemical data was performed using JMP (SAS Institute, Inc., Cary, NC, USA). We conducted a one-way ANOVA on tree means to evaluate the significance of variation of the various physiognomic and geochemical variables among treatment groups and used linear regression to assess how different characteristics vary depending on light availability.

Several multiple linear regression models for reconstructing light availability were developed using JMP. Three different models were developed based on the different types of data collected: 1) a model with all data, 2) a model with only physiognomic data, and 3) a model with physiognomic and isotopic data. These three iterations were developed due to the differences in fossil leaf preservation caused by variations in taphonomic processes after burial. We used stepwise linear regression to find the best-fit models for each of the three different suites of variables. To choose the best models, we excluded variables that were collinear from our models. We then used a combination of  $r^2$ , model standard error, goodness of fit (AIC and SSE), and the number of variables present to determine the final model.

## CHAPTER THREE

### Results

We measured various physiognomic traits, stable isotopes, and molecular component abundances for both modern and fossil leaves (Table A.1).

#### *Leaf Physiognomic Response to Light Environment*

We found a strong relationship between leaf physiognomy and light. Several leaf physiognomic traits were correlated with daily light integral (Table A.5). In particular, we found both negative and positive relationships between DLI and several variables (Figure 3.1), such as negative correlations with perimeter ( $r^2 = 0.87$ ,  $P = 0.0067$ ) and leaf area ( $r^2 = 0.73$ ,  $P = 0.03$ ) (Figure 3.1A, B), and a positive correlation with number of teeth:internal perimeter ( $r^2 = 0.22$ ,  $P = 0.35$ ) (Figure 3.1F). Further, we found that several leaf physiognomic traits were significantly different between light treatments (Figure 3.2). For example, in the trait leaf perimeter, the control and the 30% black shade cloth groups were significantly different than the other groups, the 90% green shade cloth group was significantly different than the 90% black shade cloth group, and both 90% shade groups were each indistinguishable from both the 60% black and the 60% green shade cloth groups (Figure 3.2A). Similarly, with leaf area, the control and the 30% black shade cloth groups were significantly different than the other groups, the 60% black shade cloth group was significantly different than the 60% green shade cloth group, and both 60% light treatment were significantly different from the 90% green or the 90% black shade cloth groups

(Figure 3.2B). However, for some traits, there were no significant differences between light treatments (Figure 3.2C, D, F).

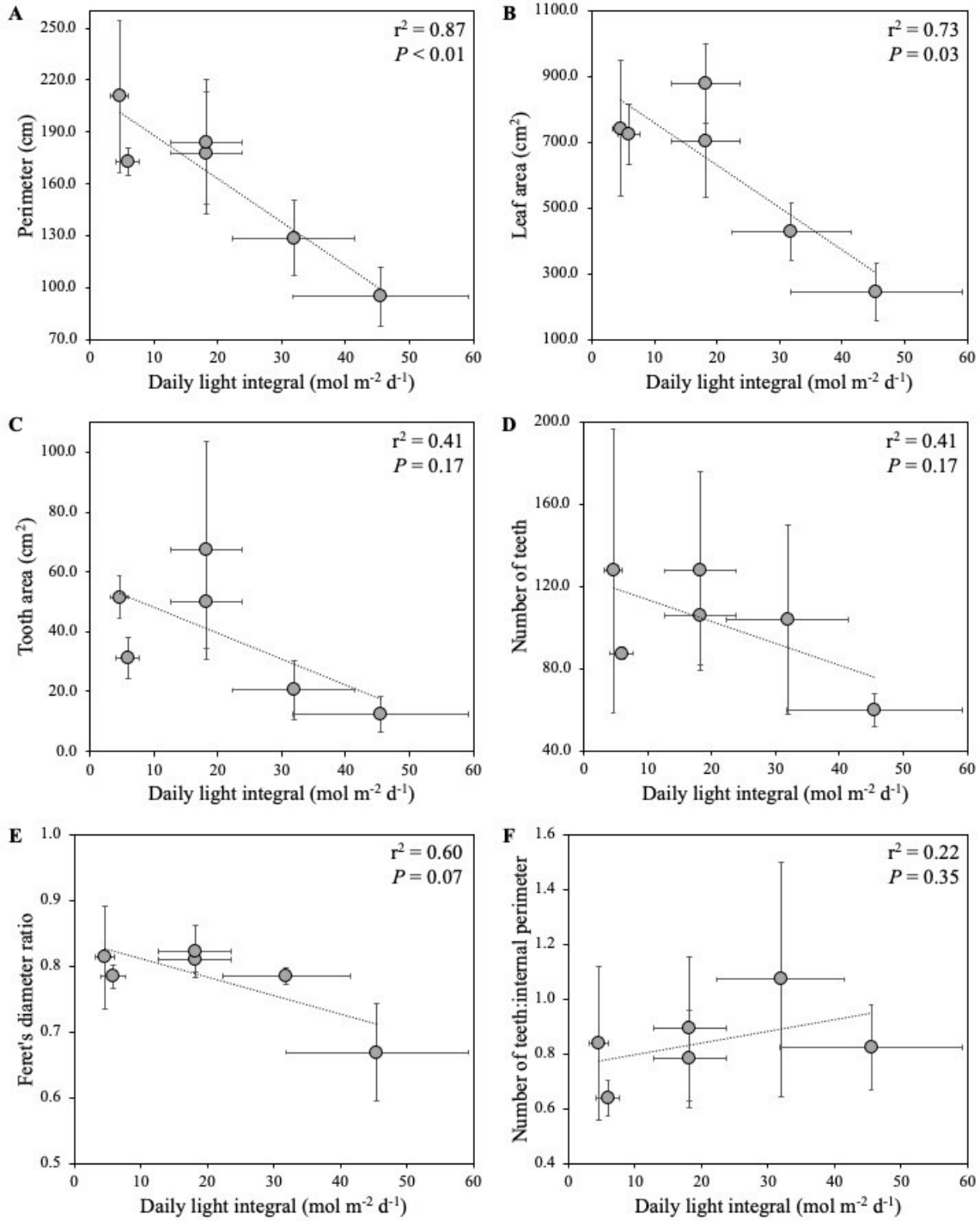


Figure 3.1. Relationship between light treatment and leaf physiognomic traits. The standard deviation of each group mean is plotted.

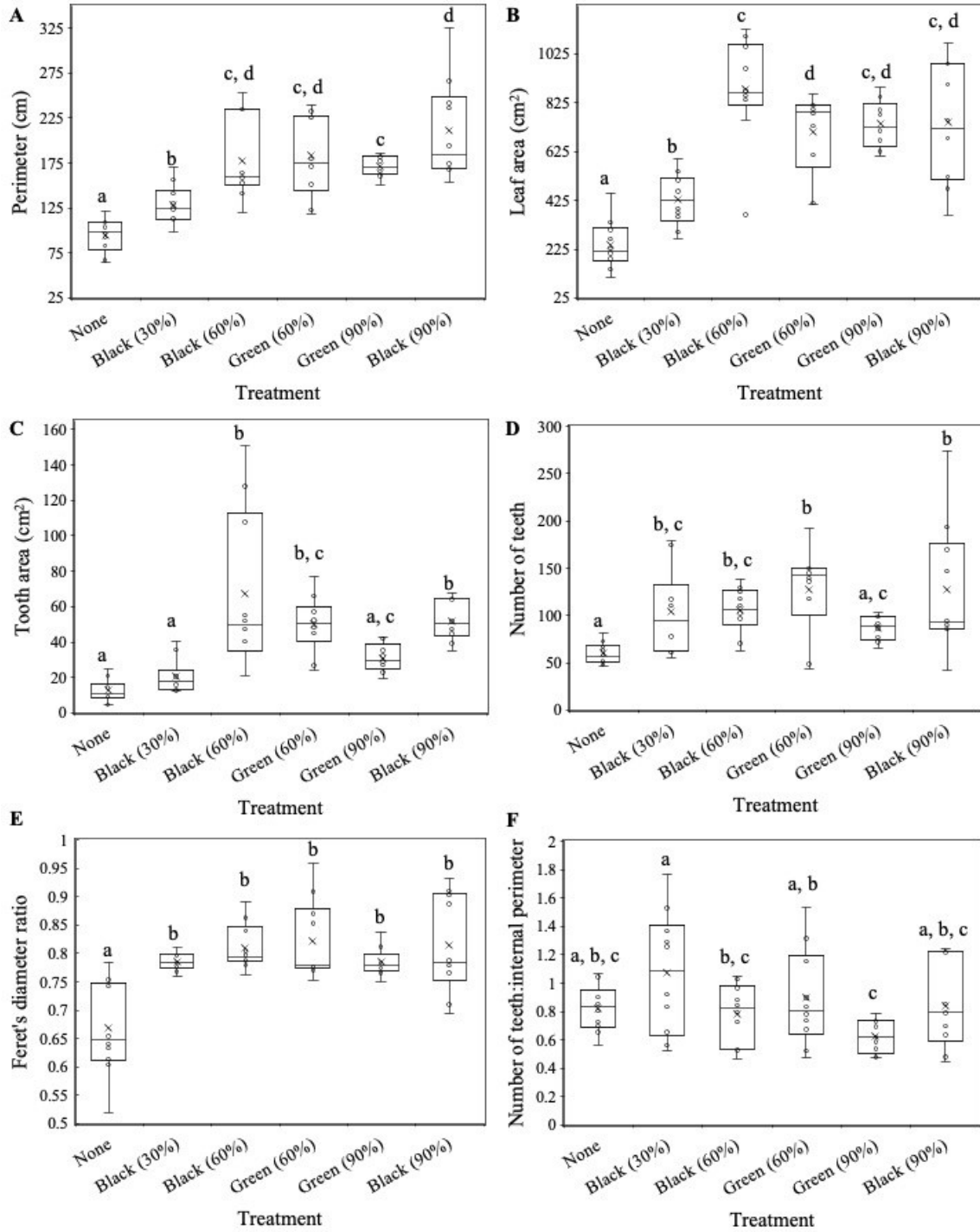


Figure 3.2. Relationship between light treatment and leaf physiognomic traits. Boxplots are on the individual leaf level. For multiple comparisons, a significant difference exists between treatment types that are not connected by the same letter, at the 0.05 level.

### *Leaf Molecular Structure Response to Light Environment*

Of the five molecular components of modern leaves that can be estimated by using peak areas from  $^{13}\text{C}$  NMR, only lignin and lipids can be successfully detected in fossil leaves. Thus, we focused our analyses on these two molecular components. We found a significant positive correlation between DLI and lignin content of the leaves ( $r^2 = 0.97$ ,  $P = 0.0003$ ) (Figure 3.3A) and a negative correlation between DLI and lipids ( $r^2 = 0.62$ ,  $P = 0.06$ ) (Figure 3.3C). We found significant differences in lignin content based on light treatment (Figure 3.3B). Three treatment groups were significantly different from all others: no shade cloth, 30% black shade cloth, and 90% shade cloth (Figure 3.3B). The remaining three treatment groups, 60% black shade cloth, 60% green shade cloth, and 90% green shade cloth, were all statistically indistinguishable from one another (Figure 3.3B). There were no significant differences in lipid content based on light treatment (Figure 3.3D).

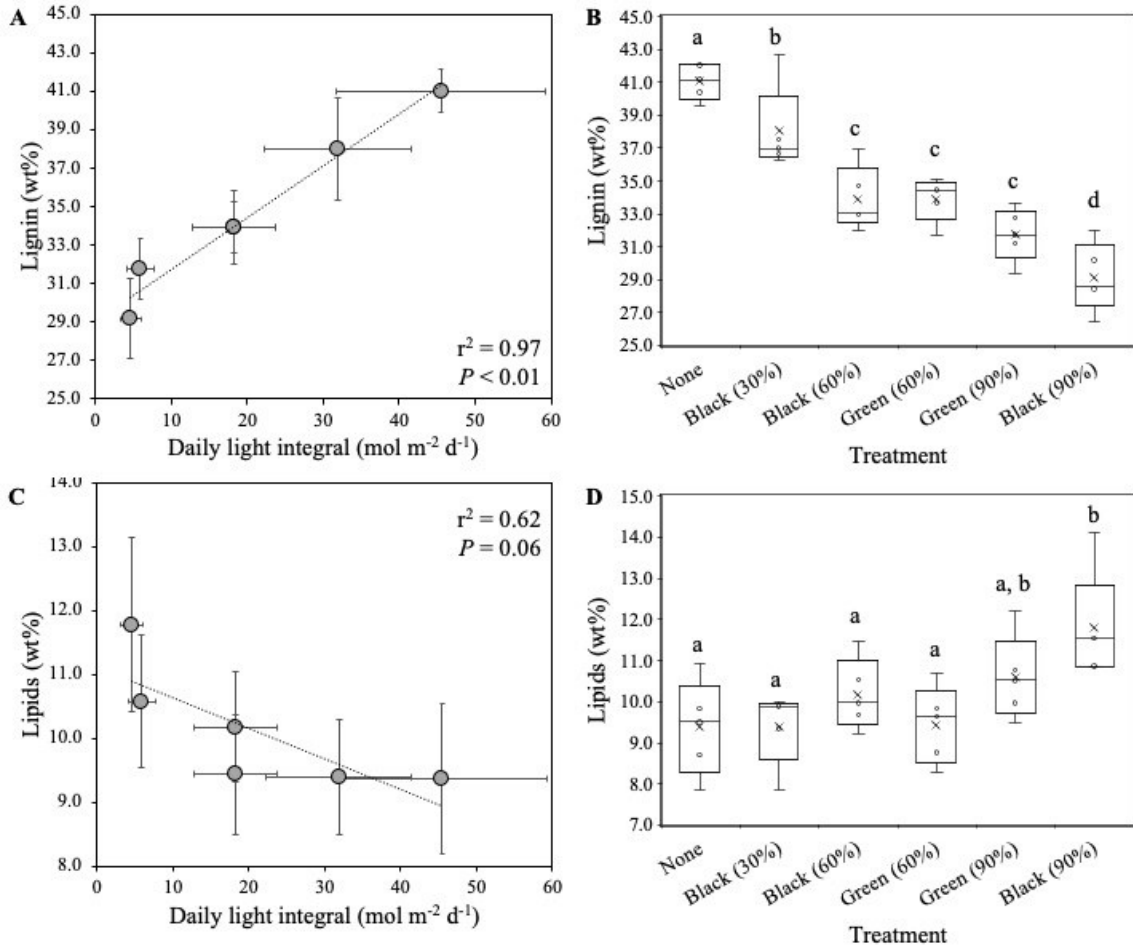


Figure 3.3. Relationship between light treatment and leaf molecular components. For linear regression of daily light integral and leaf molecular components (A, C), standard deviation of each group mean is plotted. Boxplots (B, D) are on the individual tree level. For multiple comparisons, a significant difference exists between treatment types that are not connected by the same letter, at the 0.05 level.

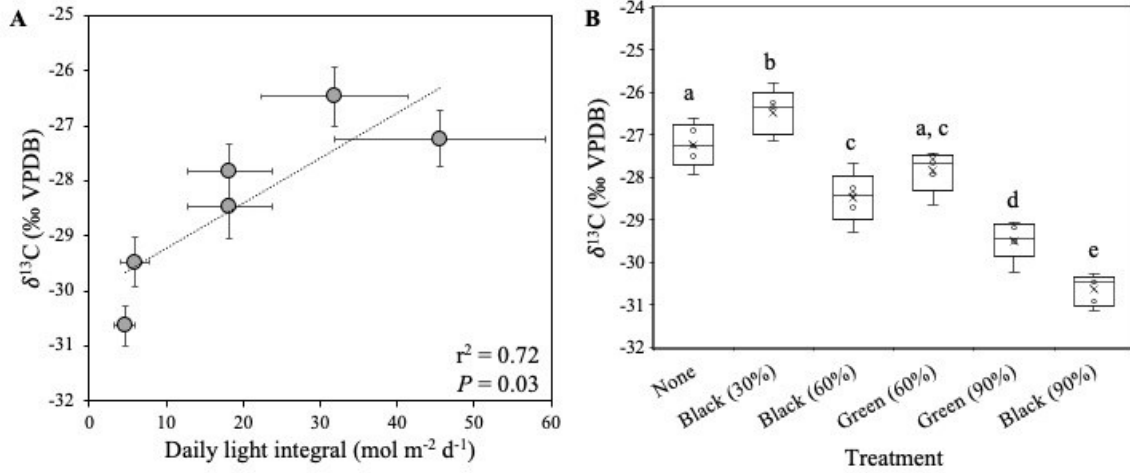


Figure 3.4. Relationship between light treatment and leaf  $\delta^{13}\text{C}$ . (A) Linear regression of daily light integral and  $\delta^{13}\text{C}$ . Standard deviation of each group mean is plotted. Boxplot (B) is on the individual tree level. For multiple comparisons, a significant difference exists between treatment types that are not connected by the same letter, at the 0.05 level.

### *Leaf $\delta^{13}\text{C}$ Response to Light Environment*

We found a significant positive correlation between DLI and leaf  $\delta^{13}\text{C}$  ( $r^2 = 0.72$ ,  $P = 0.03$ ) (Figure 3.4A). Additionally, we found significant differences in leaf  $\delta^{13}\text{C}$  based on light treatment for certain treatment groups (Figure 3.4B). The 60% green shade group was statistically indistinguishable from both the no shade cloth and the 60% black shade cloth groups (Figure 3.4B). The 30% black shade cloth, 90% green shade cloth, and 90% black shade cloth groups were all significantly different from one another and from all other treatment groups (Figure 3.4B).

### *Predictive DLI Linear Regression*

Using the suite of physiognomic and geochemical variables and their relationships with DLI, we developed three different multiple linear regression models that have the potential to be used to estimate DLI (Table 3.1). In our model selection criteria, we defined our ‘best model’ as one that had a minimal number of characters and had the lowest AIC, highest  $r^2$ , and lowest SE. First, the best model overall (model 1; AIC = 195.9,  $r^2 = 0.9$ , SE =  $5.5 \text{ mol m}^{-2} \text{ d}^{-1}$ ), which considers all potential variables, included lignin, number of teeth:blade area, and number of teeth:internal perimeter (Table 3.1). This model is ideal for estimating DLI at fossil sites where leaves are preserved almost entirely, with ample cuticle and good margins. Second, the best model which only considers physiognomic variables (model 2; AIC = 219.6,  $r^2 = 0.7$ , SE =  $7.9 \text{ mol m}^{-2} \text{ d}^{-1}$ ) included leaf area, tooth area:internal perimeter, perimeter ratio, and number of teeth:blade area (Table 3.1). This model is ideal for estimating DLI at fossil sites where leaves have little to no organic material preserved. Last, the best model which considers all variables except those from

NMR (model 3; AIC = 209.7,  $r^2 = 0.8$ , SE = 6.9 mol m<sup>-2</sup> d<sup>-1</sup>) included  $\delta^{13}\text{C}$ , feret's diameter ratio, and number of teeth:perimeter (Table 3.1). This model is ideal for estimating DLI at fossil sites where leaves have just enough organic material preserved to successfully measure  $\delta^{13}\text{C}$ , but not preserved cuticle for NMR analysis, and have good margins for physiognomic measurements.

#### *Reconstructed DLI from Fossil Platanites*

We used the three multiple linear regression models constructed to estimate DLI at site DP-1304 in the San Juan Basin, New Mexico (Table 3.1). For the purposes of estimating DLI, we used data averaged for all specimens at the site. The first model (model 1; AIC = 195.9,  $r^2 = 0.9$ , SE = 5.5 mol m<sup>-2</sup> d<sup>-1</sup>) yielded an  $r\text{DLI}$  value of 111.32±5.9 mol m<sup>-2</sup> d<sup>-1</sup>. The second model (model 2; AIC = 219.6,  $r^2 = 0.7$ , SE = 7.9 mol m<sup>-2</sup> d<sup>-1</sup>) yielded an  $r\text{DLI}$  value of 109.94±7.9 mol m<sup>-2</sup> d<sup>-1</sup>. The last model (model 3; AIC = 209.7,  $r^2 = 0.8$ , SE = 6.9 mol m<sup>-2</sup> d<sup>-1</sup>) yielded an  $r\text{DLI}$  value of 41.26±6.9 mol m<sup>-2</sup> d<sup>-1</sup>.

Table 3.1. Regression models for predicting daily light integral (DLI). Data is based on 59 leaves from Milligan et al. (2021) shade cloth experiment. Data used for constructing the models were averages at the tree level.

| Regression model  | Variables                       | Coefficient | $r^2$ | SE  | F    | $P$    | AIC   |
|---|---------------------------------|-------------|-------|-----|------|--------|-------|
| (1) Best model; all variables input                       | Lignin (wt%)                    | 2.573223    | 0.9   | 5.5 | 58.5 | <.0001 | 195.9 |
|   | Number of teeth:blade area      | 64.180349   |       |     |      |        |       |
|   | Number of teeth:internal perime | -8.74349    |       |     |      |        |       |
|   | Constant                        | -73.08679   |       |     |      |        |       |
| (2) Best model; only physiognomic variables input         | Leaf area (cm <sup>2</sup> )    | -0.049267   | 0.7   | 7.9 | 18.2 | <.0001 | 219.6 |
|   | Tooth area:internal perimeter   | 39.174191   |       |     |      |        |       |
|   | Perimeter ratio                 | -45.47584   |       |     |      |        |       |
|   | Number of teeth:blade area      | 61.83581    |       |     |      |        |       |
| (3) Best model; all variables input excluding NMR results | Constant                        | 87.720387   | 0.8   | 6.9 | 33.8 | <.0001 | 209.7 |
|   | $\delta^{13}\text{C}$ (‰ VPDB)  | 6.1464821   |       |     |      |        |       |
|   | Feret's diameter ratio          | -90.79426   |       |     |      |        |       |
|   | Number of teeth:perimeter       | 9.5999205   |       |     |      |        |       |
|   | Constant                        | 259.75242   |       |     |      |        |       |

## CHAPTER FOUR

### Discussion

#### *Influences on Leaf Traits: Climate, Light Quantity, Light Quality*

Building on the work of Milligan et al. (2021), we quantified the physiognomic and geochemical response of *Platanus occidentalis* leaves to changes in light intensity. Milligan et al. (2021) found significant negative correlations between DLI and both cell area and undulation index (UI) for either side of the leaves, abaxial and adaxial. For both abaxial and adaxial undulation index, they found significant differences based on light quantity (i.e., 0%, 30%, 60%, 90%). The results we present here show similar patterns to Milligan et al. (2021). For example, we observed significant negative correlations between DLI and both perimeter and leaf area (Figure 3.1A, B). Similar to what Milligan et al. (2021) found for both abaxial and adaxial cell area, for perimeter and leaf area we did not observe many significant differences based on light treatment – only the no shade cloth and 30% black shade cloth groups were significantly different from all other light treatments (Figure 3.2A, B). Importantly, this suggests agreement between the response of the leaf morphology to variation in light on multiple scales, both the whole leaf and the leaf cells.

Amongst the various physiognomic and geochemical variables measured here, there appear to be two main drivers in the patterns observed: 1) climate and 2) light. Paleoproxies for temperature and precipitation are based upon the relationships that exist between leaf physiognomy and climate (e.g., Peppe et al. 2011; Peppe et al. 2018). Peppe

et al. (2011) developed multiple linear regression models for predicting mean annual temperature and mean annual precipitation, based on the relationship between leaf physiognomy and climate using a method called digital leaf physiognomy (DiLP). Ideally, the physiognomic variables used in these models would primarily be responding to climatic factors, and not others like differences in light. Our work suggests that the variables used in the DiLP mean annual temperature model are not strongly influenced by light. For example, feret's diameter ratio and number of teeth:internal perimeter are two of the variables in the DiLP mean annual temperature model (Peppe et al., 2011). In our work, we found a negative correlation between DLI and feret's diameter ratio ( $r^2 = 0.60$ ,  $P = 0.07$ ) and a positive correlation between DLI and number of teeth:internal perimeter ( $r^2 = 0.22$ ,  $P = 0.35$ ) (Figure 3.1E, F). However, neither of these relationships were significant. Further, we did not observe any significant differences between light treatments for these two traits (Figure 3.2E, F). This suggests that these two physiognomic traits are at most only moderately influenced by light availability. However, our molecular and physiognomic model (model 1) includes number of teeth:internal perimeter, and our isotopic and physiognomic model (model 3) includes feret's diameter ratio (Table 3.1). This suggests that despite the weak relationships between DLI and these traits, individually, they provide important predictive power to our regression models.

Other physiognomic variables, on the other hand, appear to be influenced by both climate and light. Leaf size is one of the key traits that changes with climate, and it is used in models for precipitation (Peppe et al. 2011). Wright et al. (2017) showed that differences in leaf-to-air temperatures between day and night are a key factor influencing the geographic gradients observed in leaf size. Further, Baumgartner et al. (2020) found that

allometric and heteroblastic changes in leaf shape observed in their study were affected by changing temperature and precipitation. With our study, we show that these physiognomic traits are not only affected by climatic factors, but also by light availability (Figure 3.1; Figure 3.2). Some variables that responded to changes in DLI, for example, include perimeter, leaf area, tooth area, and number of teeth (Figure 3.1A, B, C, D). These variables exhibited a stronger relationship with DLI compared to the two aforementioned (feret's diameter ratio and number of teeth:internal perimeter). It is unclear, however, the relative influence of climate versus light availability that underlies these relationships with leaf physiognomy.

Finally, some variables appeared to be influenced more by light availability. We found that as light availability decreases, *P. occidentalis* leaves increased in area (Figure 3.1B). We also found that as light availability decreases, lignin content of *P. occidentalis* leaves decreased (Figure 3.3C). For both of these variables, we found significant differences between light treatment groups (Figure 3.2A; Figure 3.3B). This suggests that leaves exposed to higher levels of irradiance are both smaller in size and thicker, while those exposed to less irradiance would be larger and thinner, which is exactly what we saw when we analyzed the leaves qualitatively. We also found that as light availability decreases, lipid content of *P. occidentalis* leaves increased slightly (Figure 3.3C). However, this relationship was not statistically significant, and there were no significant differences between light treatment groups (Figure 3.3D).

Lastly, we consider the potential influence of light quality. In Milligan et al's (2021) outdoor shade cloth experiment, they tested the effect of both light quantity and light quality on leaf cell morphology and carbon isotopic composition. The different colored

shade cloths, black and green, were used to assess variability in light quality, with the green shade cloths mimicking low red to far red (R/FR) ratios seen in natural canopies (Smith, 1982), which can influence plant development (e.g., Griffith and Sultan, 2005). The authors reported no significant differences in any of the measured leaf traits based on light quality (Milligan et al., 2021). However, in our work, we found a significant difference in  $\delta^{13}\text{C}$  between the 90% green and black shade cloth treatments (Figure 3.4B). For lignin, we found that the 30% and 90% shade cloth groups were each distinguishable from the 60% and 90% green shade cloth groups, but the 60% black shade cloth group was not (Figure 3.3B). For the various measured physiognomic traits, we did not observe any significant differences based on light quality (Figure 3.2). This suggests that light quality influences plant biochemistry and leaf chemical structure and composition, but not morphology. Thus, the differences found in light quality suggests that leaf position in a tree and within the canopy may have an effect on geochemistry. In the future, assessments of the potential impact light quality had on specifically the geochemical traits of the leaves measured should be assessed as this may provide more insight into canopy structure.

#### *Developing Multivariate Models for Predicting Light Intensity using Modern *Platanus**

Using the suite of variables measured, we developed three multivariate models on the basis of their responses to different light environments (Table 3.1). The three iterations of the models each have their own utility based on how well fossil leaves are preserved at a given site. It is important to note that these models are species-specific, meaning they only have the capacity to be applied to fossil leaf sites with extinct relatives of *P. occidentalis* (e.g., *Platanites*). It has long been known that there are certain species-specific

responses to light availability (e.g., Messier et al., 1999), and work by Cheesman et al. (2020) and Milligan et al. (2021) demonstrates the importance of developing species-specific models.

When developing any proxy for paleoenvironments, it is important to consider outside influences that could introduce uncertainties. In a review by Jordan (2011), the author asserts that any good proxy should be protected from environmental and genetic change. In this case, we are interested in what else, other than light intensity, has an effect on a leaf's  $\delta^{13}\text{C}$ , molecular component abundances, and physiognomy. Many environmental factors (e.g., temperature, nutrient availability, water availability, altitude) and plant attributes (e.g., age, growth form, phylogeny) have an effect on the carbon isotopic composition of leaves (reviewed in Arens et al. [2000]). Additionally, the molecular makeup of leaves can be influenced by factors such as water availability (Ansari et al., 2019), tree species richness (Weinhold et al., 2022), and phenological stage (Mendez-Lopez et al., 2023). Finally, different size and shape traits of leaves correlate with different climatic variables (e.g., temperature, water availability) on different scales (e.g., global vs. local) (reviewed in Peppe et al. [2011, 2018]). Our work attempts to mitigate some of these potential confounding factors by utilizing trees grown under similar conditions, except for variations in light environments (Milligan et al., 2021).

#### *Predicted DLI at Fossil Sites and Interpretation of Light Environment*

Our estimate for lignin content in fossil *Platanites* leaves from site DP-1304 was 43.4%, which most closely matches the lignin content value for the control plot that had no shade cloth covering it (Figure 3.3A). Additionally, the average  $\delta^{13}\text{C}$  at this site was -

26.4‰. If we plot this on the regression line for  $\delta^{13}\text{C}$  of the *P. occidentalis* leaves, the value would fall closest to that of the control plot (Figure 3.4A). Based on the measured values of these geochemical variables for the fossil *Platanites* at site DP-1304, we would likely infer the leaves were exposed to high levels of irradiance. Certain physiognomic variables, like inferred leaf area and perimeter, were very low compared to the ranges found for the *P. occidentalis* leaves from the shade cloth experiment (26.9 cm<sup>2</sup> and 19.8 cm, respectively) (Figure 3.2A, B). When compared to the modern leaves, these values suggest a very high *rDLI*, and thus a very high level of irradiance, potentially even higher than that of the control plot where no shade cloth covered the trees (Figure 3.1A, B). Milligan et al. (2021) found that models using cell area and undulation index (UI) would indicate an open environment based on the high values of *rDLI* output, which is similar to what our geochemical and physiognomic data suggest. Interestingly, their model utilizing the carbon isotope discrimination in plant leaves ( $\Delta_{\text{leaf}}$ ) indicated a closed canopy as evidenced by low and negative values of *rDLI* output (Milligan et al., 2021). Here, our isotopic data seems to be in general agreement with both our molecular makeup and physiognomic data, all suggesting the leaves at site DP-1304 experienced high levels of irradiance.

It may also be possible, however, that a taphonomic bias toward sun leaves is responsible for such results. Leaves from the upper canopy have been found to be the most significant contributor to litter (Osada et al., 2001). Those same leaves are also the most likely to survive the transport to deposition phase prior to burial and fossilization (Spicer, 1981). Due to their exposure to high levels of irradiance, these upper canopy leaves are also known to have higher leaf mass per area (Koch et al., 2004; Sack et al., 2006) and thicker cuticles (Osborn and Taylor, 1990) compared to leaves from the middle and lower

canopy where irradiance levels are much lower. Both of these factors may increase the preservation potential of such leaves. It is therefore important to keep in mind the potential of taphonomic biases that could be introduced in our results when applying such models to fossil leaf sites.

Our third model, which uses  $\delta^{13}\text{C}$ , feret's diameter ratio, and number of teeth:perimeter, produced the most reasonable prediction of DLI for *Platanites* fossil leaves at site DP-1304:  $41.3 \text{ mol m}^{-2} \text{ d}^{-1}$  (Table 3.1). This  $r\text{DLI}$  value falls within the range of DLI values for the United States (Faust and Logan, 2018) and globally (Poorter et al., 2019). These values range from  $\sim 0\text{-}65 \text{ mol m}^{-2} \text{ d}^{-1}$ , depending on several factors (e.g., season, latitude, cloudiness) (Faust and Logan, 2018; Poorter et al., 2019). Additionally, our value falls within the range of  $r\text{DLI}$  of 32.94 and  $52.65 \text{ mol m}^{-2} \text{ d}^{-1}$  estimated by Milligan et al. (2021) for site DP-1304. These results demonstrate that models for light availability using 1) cell morphology and 2) carbon isotopic composition along with physiognomic traits agree. Based on the range of DLI values predicted using the three models developed here, our results are in agreement with those of Milligan et al. (2021), and suggest either 1) we sampled leaves that came mostly from the upper canopy or 2) we sampled leaves that mostly came from the forest edge within a riparian environment, where fossil Platanaceae are commonly found (Royer et al., 2003).

## CHAPTER FIVE

### Conclusions

This study quantified the response of various leaf traits (physiognomic, isotopic, molecular) in *P. occidentalis* to changes in level of irradiance. We found some traits had a significant relationship with DLI: perimeter, leaf area, lignin, and  $\delta^{13}\text{C}$ . Other traits, such as tooth area, number of teeth, and lipids showed a weaker response to changes in DLI, but still appeared to respond to such changes to some degree. Other variables, such as feret's diameter ratio and number of teeth:internal perimeter, seem to be influenced more by climatic factors than light availability. Additionally, when comparing treatment groups, certain traits showed more significant differences than others. Interestingly, we found that light quality, in addition to light quantity, may be influence some leaf traits. We developed three multivariate linear regression models for predicting DLI based on the relationships we observed between DLI and the various leaf traits measured. We applied these models to a fossil site (DP-1304) from the San Juan Basin in New Mexico, which preserves *Platanites* leaves from the early Paleocene. Based on the output from the models, we interpret that either upper canopy leaves exposed to more sunlight are being preferentially preserved or leaves on the outer edge of the forest along a riparian environment exposed to more sunlight are being preferentially preserved.

## APPENDIX

## APPENDIX

### Supplemental Data

This appendix consists of raw physiognomic and isotopic data, as well as molecular data sourced from a mixing model, which were all used as input for model building. It also includes corrected peak area data from NMR analyses, which was the input into the mixing model from which the molecular data is sourced. Lastly, there is a correlation matrix between DLI and all variables considered for the purposes of this project.

Table A.1. Physiognomic data for each individual *P. occidentalis* leaf.

| Treatment                            | DLI  | Tree | Leaf | Leaf area (cm <sup>2</sup> ) | Perimeter (cm) | Internal perimeter (cm) | # primary teeth | # secondary teeth | # teeth | Tooth area (cm <sup>2</sup> ) | Feret diameter ratio | Tooth area:perimeter | Tooth area:internal perimeter | Average tooth area (cm <sup>2</sup> ) | Tooth area:blade area | # teeth:perimeter | # teeth:internal perimeter | Perimeter ratio | # teeth:blade area |
|--------------------------------------|------|------|------|------------------------------|----------------|-------------------------|-----------------|-------------------|---------|-------------------------------|----------------------|----------------------|-------------------------------|---------------------------------------|-----------------------|-------------------|----------------------------|-----------------|--------------------|
| Control no shade cloth               | 45.5 | 1    | a    | 111.02                       | 66.88          | 53.79                   | 38.00           | 8.00              | 46.00   | 4.85                          | 0.52                 | 0.07                 | 0.09                          | 0.13                                  | 0.04                  | 0.69              | 0.86                       | 1.24            | 0.41               |
|                                      |      |      | b    | 210.75                       | 96.81          | 68.39                   | 41.00           | 32.00             | 73.00   | 10.69                         | 0.61                 | 0.11                 | 0.16                          | 0.26                                  | 0.05                  | 0.75              | 1.07                       | 1.42            | 0.35               |
|                                      |      | 2    | a    | 186.30                       | 92.45          | 64.09                   | 48.00           | 19.00             | 67.00   | 9.30                          | 0.64                 | 0.10                 | 0.15                          | 0.19                                  | 0.05                  | 0.72              | 1.05                       | 1.44            | 0.36               |
|                                      |      |      | b    | 207.74                       | 99.48          | 69.75                   | 41.00           | 22.00             | 63.00   | 10.57                         | 0.60                 | 0.11                 | 0.15                          | 0.26                                  | 0.05                  | 0.63              | 0.90                       | 1.43            | 0.30               |
|                                      |      | 3    | a    | 334.04                       | 109.04         | 83.97                   | 37.00           | 18.00             | 55.00   | 14.29                         | 0.75                 | 0.13                 | 0.17                          | 0.39                                  | 0.04                  | 0.50              | 0.65                       | 1.30            | 0.16               |
|                                      |      |      | b    | 303.69                       | 111.21         | 78.87                   | 37.00           | 18.00             | 55.00   | 21.11                         | 0.75                 | 0.19                 | 0.27                          | 0.57                                  | 0.07                  | 0.49              | 0.70                       | 1.41            | 0.18               |
|                                      |      | 4    | a    | 226.82                       | 82.89          | 64.39                   | 32.00           | 20.00             | 52.00   | 9.76                          | 0.78                 | 0.12                 | 0.15                          | 0.30                                  | 0.04                  | 0.63              | 0.81                       | 1.29            | 0.23               |
|                                      |      |      | b    | 142.34                       | 64.54          | 51.84                   | 34.00           | 14.00             | 48.00   | 4.84                          | 0.63                 | 0.07                 | 0.09                          | 0.14                                  | 0.03                  | 0.63              | 0.74                       | 0.93            | 1.24               |
|                                      |      | 5    | a    | 453.64                       | 122.05         | 144.50                  | 34.00           | 48.00             | 82.00   | 24.86                         | 0.65                 | 0.20                 | 0.17                          | 0.73                                  | 0.05                  | 0.67              | 0.57                       | 0.84            | 0.18               |
|                                      |      |      | b    | 267.70                       | 103.62         | 79.61                   | 34.00           | 24.00             | 58.00   | 14.55                         | 0.74                 | 0.14                 | 0.18                          | 0.43                                  | 0.05                  | 0.56              | 0.73                       | 1.30            | 0.22               |
| BK30: black shade cloth, 30% density | 31.9 | 1    | a    | 462.57                       | 124.16         | 107.05                  | 38.00           | 18.00             | 56.00   | 13.36                         | 0.80                 | 0.11                 | 0.12                          | 0.35                                  | 0.03                  | 0.45              | 0.52                       | 1.16            | 0.12               |
|                                      |      |      | b    | 471.13                       | 130.15         | 107.91                  | 36.00           | 25.00             | 61.00   | 17.58                         | 0.79                 | 0.14                 | 0.16                          | 0.49                                  | 0.04                  | 0.47              | 0.57                       | 1.21            | 0.13               |
|                                      |      | 2    | a    | 542.41                       | 141.41         | 118.95                  | 38.00           | 40.00             | 78.00   | 20.65                         | 0.80                 | 0.15                 | 0.17                          | 0.54                                  | 0.04                  | 0.55              | 0.66                       | 1.19            | 0.14               |
|                                      |      |      | b    | 296.23                       | 113.38         | 84.64                   | 36.00           | 42.00             | 78.00   | 12.49                         | 0.78                 | 0.11                 | 0.15                          | 0.35                                  | 0.04                  | 0.69              | 0.92                       | 1.34            | 0.26               |
|                                      |      | 3    | a    | 373.08                       | 110.85         | 85.32                   | 39.00           | 78.00             | 117.00  | 15.90                         | 0.81                 | 0.14                 | 0.19                          | 0.41                                  | 0.04                  | 1.06              | 1.37                       | 1.30            | 0.31               |
|                                      |      |      | b    | 267.97                       | 98.34          | 76.63                   | 36.00           | 28.00             | 64.00   | 12.84                         | 0.78                 | 0.13                 | 0.17                          | 0.36                                  | 0.05                  | 0.65              | 0.84                       | 1.28            | 0.24               |
|                                      |      | 4    | a    | 391.43                       | 123.62         | 92.07                   | 44.00           | 75.00             | 119.00  | 17.67                         | 0.76                 | 0.19                 | 0.40                          | 0.40                                  | 0.05                  | 0.96              | 1.29                       | 1.34            | 0.30               |
|                                      |      |      | b    | 356.32                       | 116.84         | 88.28                   | 45.00           | 66.00             | 111.00  | 17.43                         | 0.77                 | 0.15                 | 0.20                          | 0.39                                  | 0.05                  | 0.95              | 1.26                       | 1.32            | 0.31               |
|                                      |      | 5    | a    | 506.15                       | 156.88         | 101.50                  | 44.00           | 135.00            | 179.00  | 35.95                         | 0.78                 | 0.23                 | 0.20                          | 0.82                                  | 0.07                  | 1.14              | 1.76                       | 1.55            | 0.35               |
|                                      |      |      | b    | 591.34                       | 170.68         | 114.40                  | 48.00           | 127.00            | 175.00  | 40.70                         | 0.80                 | 0.24                 | 0.36                          | 0.85                                  | 0.07                  | 1.03              | 1.53                       | 1.49            | 0.30               |
| BK60: black shade cloth, 60% density | 18.2 | 1    | a    | 872.24                       | 161.89         | 136.07                  | 36.00           | 27.00             | 63.00   | 47.28                         | 0.80                 | 0.29                 | 0.35                          | 1.31                                  | 0.05                  | 0.39              | 0.46                       | 1.19            | 0.07               |
|                                      |      |      | b    | 836.31                       | 164.49         | 132.28                  | 36.00           | 35.00             | 71.00   | 55.24                         | 0.79                 | 0.34                 | 0.42                          | 1.53                                  | 0.07                  | 0.43              | 0.54                       | 1.24            | 0.08               |
|                                      |      | 2    | a    | 853.74                       | 155.95         | 126.14                  | 44.00           | 86.00             | 130.00  | 35.35                         | 0.80                 | 0.23                 | 0.28                          | 0.80                                  | 0.04                  | 0.83              | 1.03                       | 1.24            | 0.15               |
|                                      |      |      | b    | 855.11                       | 159.32         | 129.46                  | 45.00           | 80.00             | 125.00  | 40.60                         | 0.84                 | 0.25                 | 0.31                          | 0.90                                  | 0.05                  | 0.78              | 0.97                       | 1.23            | 0.15               |
|                                      |      | 3    | a    | 1126.16                      | 253.74         | 223.24                  | 40.00           | 78.00             | 118.00  | 52.06                         | 0.89                 | 0.21                 | 0.23                          | 1.30                                  | 0.05                  | 0.47              | 0.53                       | 1.14            | 0.10               |
|                                      |      |      | b    | 365.77                       | 119.30         | 92.58                   | 34.00           | 63.00             | 97.00   | 20.77                         | 0.76                 | 0.17                 | 0.22                          | 0.61                                  | 0.06                  | 0.81              | 1.05                       | 1.29            | 0.27               |
|                                      |      | 4    | a    | 1095.72                      | 234.76         | 152.90                  | 41.00           | 70.00             | 111.00  | 127.92                        | 0.79                 | 0.54                 | 0.84                          | 3.12                                  | 0.12                  | 0.47              | 0.73                       | 1.54            | 0.10               |
|                                      |      |      | b    | 1054.07                      | 235.31         | 157.41                  | 46.00           | 93.00             | 139.00  | 107.91                        | 0.78                 | 0.46                 | 0.69                          | 2.35                                  | 0.10                  | 0.59              | 0.88                       | 1.49            | 0.13               |
|                                      |      | 5    | a    | 963.08                       | 152.71         | 129.13                  | 38.00           | 65.00             | 103.00  | 150.66                        | 0.86                 | 0.99                 | 1.17                          | 3.96                                  | 0.16                  | 0.67              | 0.80                       | 1.18            | 0.11               |
|                                      |      |      | b    | 752.04                       | 141.54         | 122.07                  | 40.00           | 63.00             | 103.00  | 34.94                         | 0.79                 | 0.25                 | 0.29                          | 0.87                                  | 0.05                  | 0.73              | 0.84                       | 1.16            | 0.14               |
| GR60: green shade cloth, 60% density | 18.2 | 1    | a    | 795.95                       | 240.25         | 192.16                  | 40.00           | 110.00            | 150.00  | 66.18                         | 0.87                 | 0.28                 | 0.34                          | 1.65                                  | 0.08                  | 0.62              | 0.78                       | 1.25            | 0.19               |
|                                      |      |      | b    | 730.26                       | 171.04         | 128.14                  | 50.00           | 98.00             | 148.00  | 48.32                         | 0.78                 | 0.28                 | 0.38                          | 0.97                                  | 0.07                  | 0.87              | 1.16                       | 1.33            | 0.20               |
|                                      |      | 2    | a    | 780.78                       | 225.65         | 190.16                  | 44.00           | 96.00             | 140.00  | 52.33                         | 0.91                 | 0.23                 | 0.28                          | 1.19                                  | 0.07                  | 0.62              | 0.74                       | 1.19            | 0.18               |
|                                      |      |      | b    | 609.64                       | 151.58         | 110.18                  | 45.00           | 100.00            | 145.00  | 57.12                         | 0.78                 | 0.38                 | 0.52                          | 1.27                                  | 0.09                  | 0.96              | 1.32                       | 1.38            | 0.24               |
|                                      |      | 3    | a    | 861.47                       | 232.75         | 201.07                  | 40.00           | 96.00             | 136.00  | 77.31                         | 0.85                 | 0.33                 | 0.38                          | 1.93                                  | 0.09                  | 0.58              | 0.68                       | 1.16            | 0.16               |
|                                      |      |      | b    | 804.00                       | 179.57         | 131.60                  | 46.00           | 72.00             | 118.00  | 57.98                         | 0.78                 | 0.44                 | 1.26                          | 0.07                                  | 0.66                  | 0.90              | 1.36                       | 0.15            |                    |
|                                      |      | 4    | a    | 407.19                       | 118.97         | 92.70                   | 33.00           | 11.00             | 44.00   | 23.92                         | 0.75                 | 0.20                 | 0.26                          | 0.72                                  | 0.06                  | 0.37              | 0.47                       | 1.28            | 0.11               |
|                                      |      |      | b    | 414.07                       | 123.18         | 93.14                   | 32.00           | 17.00             | 49.00   | 26.80                         | 0.77                 | 0.22                 | 0.29                          | 0.84                                  | 0.06                  | 0.40              | 0.53                       | 1.32            | 0.12               |
|                                      |      | 5    | a    | 822.92                       | 171.39         | 125.46                  | 47.00           | 146.00            | 193.00  | 45.04                         | 0.78                 | 0.26                 | 0.36                          | 0.96                                  | 0.05                  | 1.13              | 1.54                       | 1.37            | 0.23               |
|                                      |      |      | b    | 813.94                       | 226.13         | 181.79                  | 46.00           | 106.00            | 152.00  | 46.65                         | 0.96                 | 0.21                 | 0.26                          | 1.01                                  | 0.06                  | 0.67              | 0.84                       | 1.24            | 0.19               |
| GR90: green shade cloth, 87% density | 5.9  | 1    | a    | 793.36                       | 166.15         | 193.79                  | 46.00           | 46.00             | 92.00   | 27.69                         | 0.77                 | 0.17                 | 0.14                          | 0.60                                  | 0.03                  | 0.55              | 0.47                       | 0.86            | 0.12               |
|                                      |      |      | b    | 888.55                       | 169.89         | 139.51                  | 45.00           | 42.00             | 87.00   | 19.45                         | 0.81                 | 0.11                 | 0.14                          | 0.43                                  | 0.02                  | 0.62              | 1.22                       | 1.10            |                    |
|                                      |      | 2    | a    | 669.07                       | 183.52         | 133.73                  | 47.00           | 52.00             | 99.00   | 27.39                         | 0.78                 | 0.15                 | 0.20                          | 0.58                                  | 0.04                  | 0.54              | 0.74                       | 1.37            | 0.15               |
|                                      |      |      | b    | 774.12                       | 160.62         | 131.20                  | 46.00           | 31.00             | 77.00   | 22.76                         | 0.84                 | 0.14                 | 0.17                          | 0.49                                  | 0.03                  | 0.48              | 0.59                       | 1.22            | 0.10               |
|                                      |      | 3    | a    | 711.04                       | 177.71         | 131.96                  | 46.00           | 58.00             | 104.00  | 42.19                         | 0.79                 | 0.24                 | 0.32                          | 0.92                                  | 0.06                  | 0.59              | 0.79                       | 1.35            | 0.15               |
|                                      |      |      | b    | 624.07                       | 150.25         | 150.25                  | 30.00           | 42.00             | 72.00   | 35.59                         | 0.75                 | 0.24                 | 0.24                          | 1.19                                  | 0.06                  | 0.48              | 0.48                       | 1.00            | 0.12               |
|                                      |      | 4    | a    | 605.17                       | 185.75         | 121.63                  | 44.00           | 45.00             | 89.00   | 32.41                         | 0.77                 | 0.17                 | 0.27                          | 0.74                                  | 0.05                  | 0.48              | 0.73                       | 1.53            | 0.15               |
|                                      |      |      | b    | 721.83                       | 166.08         | 122.69                  | 33.00           | 33.00             | 66.00   | 42.73                         | 0.78                 | 0.26                 | 0.35                          | 1.29                                  | 0.06                  | 0.40              | 0.54                       | 1.35            | 0.09               |
|                                      |      | 5    | a    | 847.33                       | 182.19         | 142.34                  | 36.00           | 63.00             | 99.00   | 29.37                         | 0.78                 | 0.16                 | 0.21                          | 0.82                                  | 0.03                  | 0.54              | 0.70                       | 1.28            | 0.12               |
|                                      |      |      | b    | 983.81                       | 169.40         | 135.45                  | 31.00           | 55.00             | 86.00   | 64.28                         | 0.77                 | 0.38                 | 0.47                          | 2.07                                  | 0.07                  | 0.51              | 0.63                       | 1.25            | 0.09               |
| BK90: black shade cloth, 90% density | 4.6  | 1    | a    | 989.66                       | 174.32         | 135.87                  | 39.00           | 56.00             | 95.00   | 52.63                         | 0.79                 | 0.39                 | 1.35                          | 0.05                                  | 0.54                  | 0.70              | 1.28                       | 0.10            |                    |
|                                      |      |      | b    | 679.01                       | 175.00         | 115.96                  | 43.00           | 49.00             | 92.00   | 39.16                         | 0.77                 | 0.22                 | 0.34                          | 0.91                                  | 0.06                  | 0.53              | 0.79                       | 1.51            | 0.14               |
|                                      |      | 2    | a    | 751.91                       | 242.14         | 186.68                  | 32.00           | 58.00             | 90.00   | 48.87                         | 0.90                 | 0.20                 | 0.26                          | 1.53                                  | 0.06                  | 0.37              | 0.48                       | 1.30            | 0.12               |
|                                      |      |      | b    | 365.55                       | 154.07         | 94.41                   | 27.00           | 15.00             | 42.00   | 35.15                         | 0.69                 | 0.23                 | 0.37                          | 1.30                                  | 0.10                  | 0.27              | 0.44                       | 1.63            | 0.11               |
|                                      |      | 3    | a    | 471.98                       | 194.07         | 108.76                  | 47.00           | 39.00             | 86.00   | 51.83                         | 0.71                 | 0.48                 | 1.10                          | 1.10                                  | 0.11                  | 0.44              | 0.79                       | 1.78            | 0.18               |
|                                      |      |      | b    | 1065.70                      | 325.25         | 220.50                  | 54.00           | 220.00            | 274.00  | 64.45                         | 0.89                 | 0.20                 | 0.29                          | 1.19                                  | 0.06                  | 0.84              | 1.24                       | 1.48            | 0.26               |
|                                      |      | 4    | a    | 521.27                       | 236.40         | 158.80                  | 58.00           | 136.00            | 194.00  | 44.90                         | 0.93                 | 0.19                 | 0.28                          | 0.77                                  | 0.09                  | 0.82              | 1.22                       | 1.49            | 0.37               |
|                                      |      |      | b    | 898.71                       | 266.74         | 198.68                  | 50.00           | 120.00            | 170.00  | 67.38                         | 0.91                 | 0.25                 | 0.34                          | 1.35                                  | 0.07                  | 0.64              | 0.86                       | 1.34            | 0.19               |
|                                      |      | 5    | a    | 680.66                       | 168.20         | 120.51                  | 47.00           | 100.00            | 147.00  | 47.39                         | 0.78                 | 0.28                 | 0.39                          | 1.01                                  | 0.07                  | 0.87              | 1.22                       | 1.40            | 0.22               |

Table A.2. Isotopic data for *P. occidentalis* collected at the tree level.

| Treatment                            | DLI  | Tree | <sup>13</sup> C (‰ VPDB) | <sup>15</sup> N (‰ Air N2) | C wt % | N wt % | C:N   |
|--------------------------------------|------|------|--------------------------|----------------------------|--------|--------|-------|
| Control: no shade cloth              | 45.5 | 1    | -26.89                   | 4.80                       | 46.98  | 1.62   | 29.00 |
|                                      |      | 2    | -26.61                   | 3.01                       | 44.26  | 1.70   | 26.04 |
|                                      |      | 3    | -27.49                   | 3.28                       | 46.20  | 1.45   | 31.86 |
|                                      |      | 4    | -27.25                   | 1.25                       | 45.80  | 1.53   | 29.93 |
|                                      |      | 5    | -27.93                   | 2.12                       | 47.54  | 1.57   | 30.28 |
| BK30: black shade cloth, 30% density | 31.9 | 1    | -26.22                   | 2.64                       | 45.67  | 1.96   | 23.30 |
|                                      |      | 2    | -27.12                   | 2.86                       | 42.17  | 1.62   | 26.03 |
|                                      |      | 3    | -25.77                   | 2.85                       | 46.91  | 1.98   | 23.69 |
|                                      |      | 4    | -26.35                   | 2.06                       | 47.99  | 1.72   | 27.90 |
|                                      |      | 5    | -26.87                   | 2.91                       | 46.47  | 1.77   | 26.25 |
| BK60: black shade cloth, 60% density | 18.2 | 1    | -28.69                   | 4.09                       | 45.50  | 2.34   | 19.44 |
|                                      |      | 2    | -28.40                   | 7.31                       | 43.60  | 2.00   | 21.80 |
|                                      |      | 3    | -28.25                   | 3.86                       | 43.57  | 2.20   | 19.80 |
|                                      |      | 4    | -29.30                   | 6.18                       | 44.41  | 2.01   | 22.09 |
|                                      |      | 5    | -27.68                   | 3.33                       | 44.39  | 2.04   | 21.76 |
| GR60: green shade cloth, 60% density | 18.2 | 1    | -27.65                   | 7.03                       | 42.47  | 2.04   | 20.82 |
|                                      |      | 2    | -27.42                   | 3.83                       | 43.60  | 2.03   | 21.48 |
|                                      |      | 3    | -28.66                   | 5.17                       | 43.87  | 2.38   | 18.43 |
|                                      |      | 4    | -27.49                   | 3.66                       | 44.06  | 2.32   | 18.99 |
|                                      |      | 5    | -27.92                   | 3.72                       | 44.05  | 2.18   | 20.21 |
| GR90: green shade cloth, 87% density | 5.9  | 1    | -29.18                   | 5.46                       | 43.80  | 2.33   | 18.80 |
|                                      |      | 2    | -29.49                   | 3.90                       | 43.26  | 2.16   | 20.03 |
|                                      |      | 3    | -30.24                   | 3.81                       | 41.24  | 2.16   | 19.09 |
|                                      |      | 4    | -29.04                   | 3.39                       | 41.08  | 2.11   | 19.47 |
|                                      |      | 5    | -29.42                   | 2.57                       | 44.81  | 2.23   | 20.09 |
| BK90: black shade cloth, 90% density | 4.6  | 1    | -31.12                   | 2.65                       | 42.54  | 2.65   | 16.05 |
|                                      |      | 2    | -30.41                   | 4.53                       | 44.25  | 2.49   | 17.77 |
|                                      |      | 3    | -30.46                   | 4.93                       | 42.16  | 2.06   | 20.47 |
|                                      |      | 4    | -30.25                   | 3.30                       | 42.21  | 2.70   | 15.63 |
|                                      |      | 5    | -30.91                   | 2.94                       | 43.59  | 2.96   | 14.73 |

Table A.3. Results of terrestrial molecular mixing model based on corrected peak areas from NMR for *P. occidentalis* at the tree level.

| Treatment                            | DLI  | Tree | Carbohydrate (wt%) | Protein (wt%) | Lignin (wt%) | Lipid (wt%) | Carbonyl (wt%) |
|--------------------------------------|------|------|--------------------|---------------|--------------|-------------|----------------|
| Control: no shade cloth              | 45.5 | 1    | 37.90              | 0.00          | 42.10        | 14.36       | 5.64           |
|                                      |      | 2    | 36.44              | 0.00          | 44.84        | 12.57       | 6.15           |
|                                      |      | 3    | 37.01              | 0.00          | 43.40        | 10.96       | 8.63           |
|                                      |      | 4    | 35.76              | 0.00          | 44.51        | 13.17       | 6.56           |
|                                      |      | 5    | 38.90              | 0.00          | 42.81        | 12.81       | 5.49           |
| BK30: black shade cloth, 30% density | 31.9 | 1    | 38.85              | 0.00          | 40.21        | 14.22       | 6.71           |
|                                      |      | 2    | 39.43              | 0.00          | 39.56        | 13.67       | 7.35           |
|                                      |      | 3    | 32.87              | 0.00          | 45.73        | 12.10       | 9.31           |
|                                      |      | 4    | 39.68              | 0.00          | 40.23        | 13.48       | 6.62           |
|                                      |      | 5    | 41.94              | 0.00          | 39.15        | 13.11       | 5.80           |
| BK60: black shade cloth, 60% density | 18.2 | 1    | 38.74              | 2.46          | 36.26        | 15.60       | 6.94           |
|                                      |      | 2    | 38.20              | 0.21          | 38.17        | 14.94       | 8.48           |
|                                      |      | 3    | 39.75              | 3.92          | 35.80        | 13.49       | 7.03           |
|                                      |      | 4    | 42.08              | 0.58          | 35.36        | 13.42       | 8.56           |
|                                      |      | 5    | 37.41              | 0.00          | 40.40        | 14.22       | 7.97           |
| GR60: green shade cloth, 60% density | 18.2 | 1    | 39.03              | 0.00          | 37.37        | 13.44       | 10.16          |
|                                      |      | 2    | 44.40              | 4.07          | 34.66        | 13.05       | 3.82           |
|                                      |      | 3    | 35.66              | 1.51          | 38.20        | 15.43       | 9.20           |
|                                      |      | 4    | 37.34              | 2.28          | 38.07        | 13.99       | 8.32           |
|                                      |      | 5    | 39.65              | 0.00          | 38.86        | 13.17       | 8.32           |
| GR90: green shade cloth, 87% density | 5.9  | 1    | 40.80              | 9.22          | 30.94        | 14.04       | 4.99           |
|                                      |      | 2    | 40.08              | 4.49          | 35.34        | 13.21       | 6.87           |
|                                      |      | 3    | 37.89              | 7.03          | 35.69        | 13.11       | 6.28           |
|                                      |      | 4    | 36.55              | 7.31          | 33.09        | 13.05       | 10.00          |
|                                      |      | 5    | 41.83              | 3.97          | 34.47        | 12.88       | 6.84           |
| BK90: black shade cloth, 90% density | 4.6  | 1    | 37.92              | 8.45          | 32.69        | 13.85       | 7.09           |
|                                      |      | 2    | 37.03              | 6.54          | 34.55        | 13.98       | 7.90           |
|                                      |      | 3    | 40.21              | 9.05          | 29.70        | 15.59       | 5.45           |
|                                      |      | 4    | 40.07              | 11.54         | 28.19        | 13.59       | 6.61           |
|                                      |      | 5    | 38.43              | 10.11         | 31.05        | 14.53       | 5.88           |

Table A.4. Corrected peak areas from raw NMR data for *P. occidentalis* at the tree level.

| Treatment                            | DLI  | Tree | 0-45; Alkyl | 45-60; N-Alkyl/Methoxyl | 60-95; O-Alkyl | 95-110; Di-O-Alkyl | 110-145; Aromatic | 145-165; Phenolic | 165-215; Amide/Carboxyl |
|--------------------------------------|------|------|-------------|-------------------------|----------------|--------------------|-------------------|-------------------|-------------------------|
| Control: no shade cloth              | 45.5 | 1    | 18.76       | 6.04                    | 33.10          | 12.58              | 15.66             | 7.80              | 6.06                    |
|                                      |      | 2    | 17.42       | 6.09                    | 32.28          | 12.88              | 16.72             | 8.28              | 6.33                    |
|                                      |      | 3    | 16.08       | 5.20                    | 33.00          | 12.96              | 16.49             | 8.72              | 7.55                    |
|                                      |      | 4    | 17.96       | 5.67                    | 31.75          | 12.97              | 16.34             | 8.77              | 6.54                    |
|                                      |      | 5    | 17.41       | 6.01                    | 33.79          | 13.01              | 15.71             | 8.17              | 5.89                    |
| BK30: black shade cloth, 30% density | 31.9 | 1    | 18.52       | 6.56                    | 33.86          | 12.22              | 14.86             | 7.45              | 6.53                    |
|                                      |      | 2    | 18.02       | 6.37                    | 34.36          | 12.14              | 14.47             | 7.82              | 6.81                    |
|                                      |      | 3    | 17.23       | 6.04                    | 30.08          | 12.79              | 16.76             | 9.15              | 7.96                    |
|                                      |      | 4    | 17.94       | 5.76                    | 34.53          | 12.31              | 15.06             | 7.92              | 6.49                    |
|                                      |      | 5    | 17.46       | 5.94                    | 36.06          | 12.30              | 14.65             | 7.60              | 6.00                    |
| BK60: black shade cloth, 60% density | 18.2 | 1    | 20.40       | 6.98                    | 33.71          | 10.80              | 13.95             | 6.73              | 7.43                    |
|                                      |      | 2    | 19.25       | 6.69                    | 33.79          | 11.00              | 14.63             | 7.04              | 7.60                    |
|                                      |      | 3    | 19.04       | 7.17                    | 34.42          | 10.93              | 14.23             | 6.36              | 7.84                    |
|                                      |      | 4    | 17.78       | 6.39                    | 36.32          | 11.85              | 13.36             | 6.78              | 7.52                    |
|                                      |      | 5    | 18.69       | 6.38                    | 33.23          | 11.49              | 15.48             | 7.43              | 7.30                    |
| GR60: green shade cloth, 60% density | 18.2 | 1    | 17.84       | 6.39                    | 34.40          | 11.84              | 14.09             | 7.18              | 8.27                    |
|                                      |      | 2    | 18.39       | 7.01                    | 37.17          | 11.60              | 13.36             | 6.39              | 6.07                    |
|                                      |      | 3    | 20.23       | 7.02                    | 32.07          | 10.35              | 14.98             | 6.90              | 8.45                    |
|                                      |      | 4    | 19.10       | 7.15                    | 32.95          | 11.12              | 14.60             | 7.01              | 8.07                    |
|                                      |      | 5    | 17.59       | 6.63                    | 34.75          | 11.79              | 14.58             | 7.33              | 7.32                    |
| GR90: green shade cloth, 87% density | 5.9  | 1    | 21.00       | 7.74                    | 34.57          | 9.78               | 13.35             | 5.23              | 8.34                    |
|                                      |      | 2    | 18.99       | 7.19                    | 34.67          | 10.78              | 14.46             | 5.97              | 7.94                    |
|                                      |      | 3    | 19.84       | 7.82                    | 33.18          | 9.60               | 15.11             | 5.96              | 8.50                    |
|                                      |      | 4    | 19.95       | 7.65                    | 32.45          | 9.51               | 14.34             | 5.61              | 10.50                   |
|                                      |      | 5    | 18.47       | 7.02                    | 36.11          | 10.28              | 14.01             | 6.35              | 7.76                    |
| BK90: black shade cloth, 90% density | 4.6  | 1    | 20.89       | 7.80                    | 33.17          | 8.94               | 14.49             | 5.36              | 9.36                    |
|                                      |      | 2    | 20.52       | 7.59                    | 32.88          | 8.99               | 15.15             | 5.59              | 9.29                    |
|                                      |      | 3    | 22.30       | 7.67                    | 34.44          | 8.44               | 12.99             | 5.52              | 8.65                    |
|                                      |      | 4    | 21.44       | 7.94                    | 34.28          | 8.62               | 13.25             | 4.56              | 9.92                    |
|                                      |      | 5    | 21.87       | 7.95                    | 33.19          | 8.78               | 14.06             | 4.94              | 9.20                    |

Table A.5. Correlation matrix between DLI and all variables used to build predictive models. Bold values indicate a significant correlation exists between variables.

| correlation matrix                    |  |
|---------------------------------------|--|
|                                       | Daily light integral<br>(mol m <sup>-2</sup> d <sup>-1</sup> ) |
| Leaf area (cm <sup>2</sup> )          | <b>0.75</b>  |
| Perimeter (cm)                        | <b>0.77</b>  |
| Internal perimeter (cm)               | <b>0.75</b>  |
| Number of primary teeth               | <b>0.28</b>  |
| Number of secondary teeth             | <b>0.35</b>  |
| Number of teeth                       | <b>0.35</b>  |
| Tooth area (cm <sup>2</sup> )         | <b>0.50</b>  |
| Feret's diameter ratio                | <b>0.60</b>  |
| Tooth area:perimeter                  | <b>0.37</b>  |
| Tooth area:internal perimeter         | <b>0.39</b>  |
| Average tooth area (cm <sup>2</sup> ) | <b>0.49</b>  |
| Tooth area:blade area                 | <b>0.27</b>  |
| Number of teeth:perimeter             | <b>0.30</b>  |
| Number of teeth:internal perimeter    | <b>0.23</b>  |
| Perimeter ratio                       | <b>0.15</b>  |
| Number of teeth:blade area            | <b>0.59</b>  |
| Lignin (wt%)                          | <b>0.89</b>  |
| Lipids (wt%)                          | <b>0.38</b>  |
| <sup>13</sup> C (‰ VPDB)              | <b>0.81</b>  |

## BIBLIOGRAPHY

- Adams, J. M., W. A. Green, and Y. Zhang. 2008. Leaf margins and temperature in the North American flora: recalibrating the paleoclimatic thermometer. *Global and Planetary Change* 60: 523-534.
- Ansari, W. A., N. Atri, J. Ahmad, M. I. Qureshi, B. Singh, R. Kumar, V. Rai, et al. 2019. Drought mediated physiological and molecular changes in muskmelon (*Cucumis melo* L.). *PloS one* 14(9): e0222647.
- Arens, N. C., A. H. Jahren, and R. Amundson. 2000. Can C<sub>3</sub> plants faithfully record the carbon isotopic composition of atmospheric carbon dioxide? *Paleobiology* 26: 137-164.
- Asner, G. P., J. M. Scurlock, and J. A. Hicke. 2003. Global synthesis of leaf area index observations: implications for ecological and remote sensing studies. *Global Ecology and Biogeography* 12: 191-205.
- Bailey, I. W., and E. W. Sinnott. 1915. A botanical index of Cretaceous and Tertiary climates. *Science* 41: 831-834.
- Baldock, J. A., Masiello, C. A., Gelinas, Y., and Hedges, J. I. 2004. Cycling and composition of organic matter in terrestrial and marine ecosystems. *Marine Chemistry* 92: 39-64.
- Baumgartner, A., M. Donahoo, D. H. Chitwood, and D. J. Peppe. 2020. The influences of environmental change and development on leaf shape in *Vitis*. *American Journal of Botany* 107(4): 676-688.
- Betts, R. A., P. M. Cox, S. E. Lee, and F. I. Woodward. 1997. Contrasting physiological and structural vegetation feedbacks in climate change simulations. *Nature* 387: 796-799.
- Bush, R. T., J. Wallace, E. D. Currano, B. F. Jacobs, F. A. McInerney, R. E. Dunn, and N. J. Tabor. 2017. Cell anatomy and leaf  $\delta^{13}\text{C}$  as proxies for shading and canopy structure in a Miocene forest from Ethiopia. *Paleogeography, Paleoclimatology, Paleoecology* 485: 593-604.

- Carins Murphy, M. R., G. J. Jordan, and T. J. Brodribb. 2016. Cell expansion not cell differentiation predominantly co-ordinates veins and stomata within and among herbs and woody angiosperms grown under sun and shade. *Annals of Botany* 118: 1127-1138.
- Cheesman, A. W., H. Duff, K. Hill, L. A. Cernusak, and F. A. McInerney. 2020. Isotopic and morphologic proxies for reconstructing light environment and leaf function of fossil leaves: a modern calibration in the Daintree Rainforest, Australia. *American Journal of Botany* 107: 1165-1176.
- Dilcher, D. 1973. A paleoclimatic interpretation of the Eocene floras of southeastern North America. Chapter 2, 39-59. In Graham, A. (ed.) *Vegetation and vegetational history of northern Latin America*. Elsevier, Amsterdam.
- Dunn, R. E., T. Y. Le, and C. A. Strömberg. 2015. Light environment and epidermal cell morphology in grasses. *International Journal of Plant Sciences* 176: 832-847.
- Evans, J. R., and H. Poorter. 2001. Photosynthetic acclimation of plants to growth irradiance: the relative importance of leaf area and nitrogen partitioning in maximizing carbon gain. *Plant, Cell, and Environment* 24: 755-767.
- Farquhar, G. D., J. R. Ehleringer, and K. T. Hubick. 1989. Carbon isotope discrimination and photosynthesis. *Annual Review of Plant Physiology and Plant Molecular Biology* 40: 503-537.
- Faust, J. E., and J. Logan. 2018. Daily light integral: a research review and high-resolution maps of the United States. *HortScience horts* 53(9): 1250-1257.
- Flynn, A. G. 2020. Early Paleocene fossil floras, paleoclimate, and magnetostratigraphy from the San Juan Basin, New Mexico, USA. Ph.D. dissertation, Baylor University, TX, USA.
- Flynn, A. G., A. J. Davis, T. E. Williamson, M. Heizler, C. W. Fenley IV, C. E. Leslie, R. Secord, et al. 2020. Early Paleocene Magnetostratigraphy and revised biostratigraphy of the Ojo Alamo Sandstone and Lower Nacimiento Formation, San Juan Basin, New Mexico, USA. *GSA Bulletin* 132: 2154–2174.
- Gelinas, Y., Baldock, J. A., and Hedges, J. I. 2001. Demineralization of marine and freshwater sediments for CP/MAS C-13 NMR analysis. *Organic Geochemistry* 32: 677-693.
- Graham, H. V., F. Herrera, C. Jaramillo, S. L. Wing, and K. H. Freeman. 2019. Canopy structure in Late Cretaceous and Paleocene forests as reconstructed from carbon isotope analyses of fossil leaves. *Geology* 47: 977-981.

- Graham, H. V., M. E. Patzkowsky, S. L. Wing, G. G. Parker, M. L. Fogel, and K. H. Freeman. 2014. Isotopic characteristics of canopies in simulated leaf assemblages. *Geochimica et Cosmochimica Acta* 144: 82-95.
- Griffith, T. M., and S. E. Sultan. 2005. Shade tolerance plasticity in response to neutral vs green shade cues in *Polygonum* species of contrasting ecological breadth. *New Phytologist* 166: 141-148.
- Jacobs, B. F. 2002. Estimation of low-latitude paleoclimates using fossil angiosperm leaves: examples from the Miocene Tugen Hills, Kenya. *Paleobiology* 28: 399-421.
- Jacobs, B. F. 1999. Estimation of rainfall variables from leaf characters in tropical Africa. *Palaeogeography, palaeoclimatology, palaeoecology* 145: 231-250.
- Jordan, G. J. 2011. A critical framework for the assessment of biological palaeoproxies: predicting past climate and levels of atmospheric CO<sub>2</sub> from fossil leaves. *New Phytologist* 192: 29-44.
- Koch, G. W., S. C. Sillett, G. M. Jennings, and S. D. Davis. 2004. The limits to tree height. *Nature* 428: 851-854.
- Kowalski, E. A., and D. L. Dilcher. 2003. Warmer paleotemperatures for terrestrial ecosystems. *Proceedings of the National Academy of Sciences, USA* 100: 167-170.
- Kürschner, W. M. 1997. The anatomical diversity of recent and fossil leaves of the durmast oak (*Quercus petraea* Lieblein/*Q. pseudocastanea* Goeppert) implications for their use as biosensors of paleoatmospheric CO<sub>2</sub> levels. *Review of Paleobotany and Palynology* 96: 1-30.
- Le Roux, X., T. Bariac, H. Sinoquet, B. Genty, C. Piel, A. Mariotti, C. Girardin, and P. Richard. 2001. Spatial distribution of leaf water-use efficiency and carbon isotope discrimination within an isolated tree crown. *Plant, Cell & Environment* 24: 1021-1032.
- Lynch, D. J., F. A. McInerney, L. L. Kouwenberg, and M. A. Gonzalez-Meler. 2012. Plasticity in bundle sheath extensions of heterobaric leaves. *American Journal of Botany* 99: 1197-1206.
- Mendez-Lopez, A., L. del C. Lagunes-Espinoza, A. R. González-Esquinca, E. Hernández-Nataren, and C. F. Ortiz-García. 2023. Phenological characterization of chipilín (*Crotalaria longirostrata* Hook. & Arn.) and relationship between the phenological stage and chemical composition of leaves. *South African Journal of Botany* 154: 140-148.

- Messier, C., R. Doucet, J.-C. Ruel, Y. Claveau, C. Kelly, and M. J. Lechowicz. 1999. Functional ecology of advance regeneration in relation to light in boreal forests. *Canadian Journal of Forest Research* 29: 812-823.
- Milligan, J. N., A. G. Flynn, J. D. Wagner, L. L. R. Kouwenberg, R. S. Barclay, B. W. Byars, R. E. Dunn, et al. 2021. Quantifying the effect of shade on cuticle morphology and carbon isotopes of sycamores: present and past. *American Journal of Botany* 108: 2435-2451.
- Niinemets, Ü. 1999. Energy requirement for foliage formation is not constant along canopy light gradients in temperate deciduous trees. *New Phytologist* 141: 459-470.
- Nguyen Tu, T. T., W. M. Kürschner, S. Schouten, and P. F. Van Bergen. 2004. Leaf carbon isotope composition of fossil and extant oaks grown under differing atmospheric CO<sup>2</sup> levels. *Palaeogeography, Palaeoclimatology, Palaeoecology* 212: 199-213.
- Osada, N., H. Takeda, A. Furukawa, and M. Awang. 2001. Leaf dynamics and maintenance of tree crowns in a Malaysian rain forest stand. *Journal of Ecology* 89: 774-782.
- Osborn, J. M., and T. N. Taylor. 1990. Morphological and ultrastructural studies of plant cuticular membranes. I. Sun and shade leaves of *Quercus velutina* (Fagaceae). *Botanical Gazette* 151: 465-476.
- Pepper, D. J., A. Baumgartner, A. Flynn, and B. Blonder. 2018. Reconstructing paleoclimate and paleoecology using fossil leaves. In *Methods in Paleoecology: Reconstructing Cenozoic terrestrial environments and ecological communities*. Springer (Vertebrate Paleobiology and Paleoanthropology Series): 289-318.
- Peppe, D. J., D. L. Royer, B. Cariglino, S. Y. Oliver, S. Newman, E. Leight, G. Enikolopov, et al. 2011. Sensitivity of leaf size and shape to climate: global patterns and paleoclimatic applications. *New Phytologist* 190: 724-739.
- Poorter, H., Ü. Niinemets, N. Ntagkas, A. Siebenkäs, M. Mäenpää, S. Matsubara, and T. Pons. 2019. A meta-analysis of plant responses to light intensity for 70 traits ranging from molecules to whole plants performance. *New Phytologist* 223: 1073-1105.
- Poorter, H., S. Pepin, T. Rijkers, Y. de Jong, J. R. Evans, and C. Kömer. 2006. Construction costs, chemical composition and payback time of high- and low-irradiance leaves. *Journal of Experimental Botany*. 2: 355-371.
- Royer, D. L., P. Wilf, D. A. Janesko, E. A. Kowalski, and D. L. Dilcher. 2005. Correlations of climate and plant ecology to leaf size and shape: potential proxies for the fossil record. *American Journal of Botany* 92: 1141-1151.

- Royer, D. L., L. J. Hickey, and S. L. Wing. 2003. Ecological conservatism in the “living fossil” Ginkgo. *Paleobiology* 29: 84–104.
- Sack, L., P. J. Melcher, W. H. Liu, E. Middleton, and T. Pardee. 2006. How strong is intracanopy leaf plasticity in temperate deciduous trees? *American Journal of Botany* 93: 829–839.
- Smith, H. 1982. Light quality, photoperception, and plant strategy. *Annual Review of Plant Physiology* 33: 481–518.
- Spicer, R. A. 1981. The sorting and deposition of allochthonous plant material in a modern environment at Silwood Lake, Silwood Park, Berkshire, England. *U.S. Geological Survey Professional Paper* 1143: 1–77.
- Traiser, C., S. Klotz, D. Uhl, and V. Mosbrugger. 2005. Environmental signals from leaves – a physiognomic analysis of European vegetation. *New Phytologist* 166: 465–484.
- Turney, C. S. M., J. E. Hunt, and C. Burrows. 2002. Deriving a consistent  $\delta^{13}\text{C}$  signature from tree canopy leaf material for palaeoclimatic reconstruction. *New Phytologist* 155: 301–311.
- Vogel, J. C. 1978. Recycling of carbon in a forest environment. *Oecol Plant* 13: 89–94.
- Wang, Y., A. Ito, Y.-J. Huang, T. Fukushima, N. Wakamatsu, and A. Momohara. 2018. Reconstruction of altitudinal transportation range of leaves based on stomatal evidence: an example of the Early Pleistocene *Fagus* leaf fossils from central Japan. *Palaeogeography, Palaeoclimatology, Palaeoecology* 505: 317–325.
- Wang, Z., J. White, and W. Hockaday. 20XX. Changes in molecular composition of leaf lipids with seasonal gradients in temperature and light among deciduous and evergreen trees in a sub-humid ecosystem. In prep.
- Waring, R. H., A. J. S. McDonald, S. Larsson, T. Ericsson, A. Wiren, E. Arwidsson, and T. Lohammar. 1985. Differences in chemical composition of plants grown at constant relative growth rates with stable mineral nutrition. *Oecologia* 66: 157–160.
- Watson, R. W. 1942. The mechanism of elongation in palisade cells. *New Phytologist* 41: 206–221.
- Weinhold, A., S. Döll, M. Liu, A. Schedl, Y. Pöschl, X. Xu, S. Neumann, et al. 2022. Tree species richness differentially affects the chemical composition of leaves, roots and root exudates in four subtropical tree species. *Journal of Ecology* 110: 97–116.
- Wilf, P. 1997. When are leaves good thermometers? A new case for leaf margin analysis. *Paleobiology* 23: 373–390.

- Wilf, P., S. L. Wing, D. R. Greenwood, and C. L. Greenwood. 1998. Using fossil leaves as paleoprecipitation indicators: an Eocene example. *Geology* 26: 203-206.
- Wing, S., and D. R. Greenwood. 1993. Fossils and fossil climate: the case of equable continental interiors in the Eocene. *Philosophical Transactions of the Royal Society of London B* 341: 243-252.
- Wolfe, J. A. 1995. Paleoclimatic estimates from Tertiary leaf assemblages. *Annual Review of Earth and Planetary Sciences* 23: 119-142.
- Wolfe, J. A. 1993. A method of obtaining climatic parameters from leaf assemblages. *United States Geological Survey Bulletin* 2040: 1-71.
- Wright, I. J., N. Dong, V. Maire, I. C. Prentice, M. Westoby, S. Díaz, R. V. Gallagher, et al. 2017. Global climatic drivers of leaf size. *Science* 357: 917-921.
- Wu, J., B. Sun, Y.-S. C. Liu, S. Xie, and Z. Lin. 2009. A new species of *Exbucklandia* (Hamamelidaceae) from the Pliocene of China and its paleoclimatic significance. *Review of Palaeobotany and Palynology* 155: 32-41.
- Xiao, L. A., B. N. Sun, X. C. Li., W. X. Ren, and H. Jia. 2011. Anatomical variations of living and fossil *Liquidambar* leaves: a proxy for paleoenvironmental reconstruction. *Science China Earth Sciences* 54: 493-508.
- Xiao, L., H. Yang, B. Sun, X. Li, and J. Guo. 2013. Stable isotope compositions of recent and fossil sun/shade leaves and implications for palaeoenvironmental reconstruction. *Review of Palaeobotany and Palynology* 190: 75-84.